RSC Advances

PAPER

View Article Online
View Journal | View Issue

Cite this: *RSC Adv.*, 2017, **7**, 32488

Visible light sensitization of TiO_2 nanoparticles by a dietary pigment, curcumin, for environmental photochemical transformations†

Jonghun Lim, Alok D. Bokare ‡ and Wonyong Choi *

The use of curcumin, an active ingredient of turmeric powder (a dye component in curry), as a TiO_2 photosensitizer was investigated in terms of the photochemical and photoelectrochemical (PEC) properties. Owing to its strong visible light absorption and strong surface complexation, the curcumin-sensitized TiO_2 composite exhibited notable activities for the photochemical degradation of organic compounds, the reduction of chromate (Cr(VI)), and the generation of OH radicals and H_2O_2 through the reduction of O_2 under visible light (λ > 420 nm). Various spectroscopic methods confirmed the anchoring of curcumin on TiO_2 and the photochemical and PEC properties of curcumin/TiO_2 were compared with those of TiO_2 sensitized by a ruthenium complex (RuL_3) that has been frequently employed as a visible light sensitizer. Curcumin/TiO_2 exhibited consistently higher photochemical and PEC activities than RuL_3/TiO_2 over a wide pH range in an aquatic environment. These results confirm the practical viability of using a natural food dye, curcumin, as an efficient, eco-friendly, and cheap photo-sensitizer of TiO_2 for solar environmental applications. However, it should be noted that curcumin on TiO_2 like other dye sensitizers is degraded as a result of the sensitizing reactions in water and should be considered as a sensitizing reagent, not a photocatalyst.

Received 10th May 2017
Accepted 12th June 2017

DOI: 10.1039/c7ra05276f

rsc.li/rsc-advances

Introduction

Titanium dioxide (TiO_2) is one of the most popular photocatalysts, but it suffers from a lack of visible light absorption because of a large bandgap (~3 eV).[1–3] Various strategies have been attempted to increase the visible light absorption of wide bandgap semiconductors such as doping with metal or non-metal elements,[4–8] surface deposition of noble metals for plasmon effects,[9–11] and coupling with smaller bandgap semiconductors,[12–14] quantum dots[15,16] and dyes.[17–19] Among them, dye sensitization has been successfully demonstrated for many applications such as photocatalytic hydrogen production[20,21] and dye-sensitized solar cells.[22] In particular, ruthenium-based dyes have been widely used because of their high visible light absorption efficiency and stability in acidic aquatic environments.[23,24] However, it is not economical and environmentally benign, because ruthenium is not only expensive but also hazardous. Therefore, many researchers have synthesized organic dye sensitizers to replace the Ru-based dyes. Although various organic dyes have been successfully synthesized and tested for their photosensitizing effects,[18,25,26] the complex synthetic procedures and long processing time of dye preparation are serious drawbacks.

Curcumin, a natural ingredient (1.8–2.0%) in commercial turmeric powder, is a yellow pigment that is widely used as food additive and supplement. The chemical structure of curcumin consists of two phenolic groups which are connected by two α,β-unsaturated carbonyl groups exhibiting keto–enol tautomerism (see Scheme 1 for the molecular structure). It has been used in various research fields of physics, chemistry, biology and

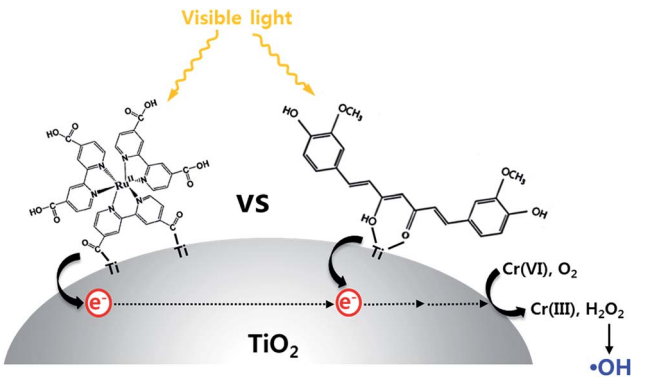

Scheme 1 Schematic illustration of the structure of curcumin-complexed TiO_2 *vs.* RuL_3-complexed TiO_2 (compared as a control).

Division of Environmental Science and Engineering, Pohang University of Science and Technology (POSTECH), Pohang 37673, Korea. E-mail: wchoi@postech.edu; Fax: +82-54-279-8299

† Electronic supplementary information (ESI) available. See DOI: 10.1039/c7ra05276f

‡ In memory of Dr. Alok D. Bokare.

medicine because of its non-toxicity, biocompatibility, and natural occurrence.[27–32] The photo-physical and photo-chemical properties of curcumin have been applied for medicinal applications such as skin protection[27] and energy applications like dye-sensitized solar cells.[33] In the case of dye-sensitized solar cell using curcumin dye, the conversion efficiency (about 1%) was much lower than that obtained using Ru-based dye.[33] However, we note that the environmentally benign nature of curcumin makes it an ideal dye sensitizer for environmental photochemical conversions that work under visible light, which has not been investigated yet. Owing to its eco-friendly properties (non-toxic nature, biocompatibility and natural occurrence), curcumin offers a much better practical alternative to any organometallic dyes including Ru-based complexes.

In this work, we investigated the use of curcumin-sensitized TiO_2 for eco-friendly photochemical applications. The curcumin sensitizer was successfully adsorbed on the TiO_2 surface in aqueous suspension and the dye–TiO_2 composite was characterized by various spectroscopic and electrochemical analyses. Under visible light ($\lambda > 420$ nm) irradiation, the photochemical and photoelectrochemical (PEC) properties of curcumin/TiO_2 were compared with a traditional ruthenium-dye/TiO_2 system. The curcumin/TiO_2 system not only showed enhanced photochemical and PEC properties, but also exhibited superior stability in water over a wide pH range.

Experimental

Materials and chemicals

TiO_2 powder (P25), a mixture of anatase and rutile (8 : 2) with a BET surface area of $\sim$50 m^2 g^{-1} and primary particle size of 20–30 nm, was used as a base catalyst material. Commercial curcumin powder (Acros Organics) was employed as the sensitizer. Ru^{II}(4,4-bipyridine-dicarboxylic acid) (RuL_3) was synthesized according to our previous method[24] and compared as a control dye throughout the study. The chemicals used in this work were $Na_2Cr_2O_7$ (Cr(VI), Aldrich), dichloroacetate (DCA, Aldrich), tetramethylammonium chloride (TMA, Acros), *tert*-butanol (*t*-BuOH, Aldrich), coumarin (Sigma), ethanol (94.5%, SAMCHUN), 5,5-dimethyl-1-pyrroline-*N*-oxide (DMPO, Sigma-Aldrich), sodium perchlorate (98%, Aldrich), and polyethylene glycol (PEG, Aldrich, molecular weight 20 kDa). All reagents were used as received.

Sample preparation

The adsorption of dye (curcumin or RuL_3) on TiO_2 surface was done in acidic aqueous suspension. TiO_2 powder (0.1 g) was dispersed in 10 mL aqueous dye solution (RuL_3 and curcumin was dissolved in deionized water and ethanol, respectively) at pH 3. Several concentrations (25, 50, 75, and 100 μM) of curcumin were tested and the optimal concentration was determined at 50 μM. The solution was stirred for 3 h, and then the dye/TiO_2 sample was collected by filtering. After drying in an oven (85 °C), orange colored powder of dye/TiO_2 was obtained.

Characterization of photocatalysts

Diffuse reflectance UV/visible absorption spectra were obtained using a spectrophotometer (Shimadzu UV-2401 PC) with an integrating sphere attachment and $BaSO_4$ was used as the reference. The surface chemical composition of curcumin/TiO_2 was determined by X-ray photoelectron spectroscopy (XPS) (Kratos XSAM 800 pci) using the Mg Kα line (1253.6 eV) as the excitation source. The binding energies of all peaks were referenced to the C 1s line (284.6 eV). The presence and distribution of C and Ti elements in the curcumin/TiO_2 particles were confirmed using a high-resolution transmission electron microscope (HR-TEM, JEM-2100F microscope with Cs-correction). FT-IR spectra were measured using thin sample pellets (referenced against a KBr pellet) on a Bomen DA8 FT-IR spectrophotometer. The photoluminescence emission spectra of curcumin were measured using a spectrofluorometer (HORIBA, Fluoromax 4C-TCSPC).

Photochemical activity test

The visible light activities of TiO_2 sensitized by curcumin and Ru-dye were tested for the reduction of chromate (Cr(VI)) and the degradation of dichloroacetate (DCA) and tetramethylammonium (TMA). The catalyst sample was dispersed in distilled water (0.5 g L^{-1}) and an aliquot of the substrate stock solution was subsequently added to the suspension to give a desired substrate concentration. The initial pH of the suspension was adjusted to 3 with $HClO_4$ standard solution for the reduction of Cr(VI) and the degradation of DCA and TMA. The light source employed was a 300 W Xe arc lamp (Oriel). Light from the source passed through a 10 cm IR water filter and a UV cutoff filter transmitting ($\lambda > 420$ nm for visible light irradiation) and then was focused onto a 30 mL Pyrex reactor with a quartz window.

Sample aliquots were withdrawn from the reactor at a given time interval during the irradiation and filtered through a 0.45 μm PTFE syringe filter (Millipore) to remove the powder samples prior to analysis. The concentrations of ionic substrates and products were quantitatively analyzed using an ion chromatograph (IC, Dionex DX-120) that was equipped with a conductivity detector and Dionex Ionpac CS-14 (4 mm × 250 mm) for cation (TMA) analysis or AS-14 (4 mm × 250 mm) column for anion (DCA and Cl^-) analysis. For the cation analysis, 10 mM methanesulfonic acid was used and 3.5 mM Na_2CO_3/1 mM $NaHCO_3$ was used for the anion analysis. The concentration of Cr(VI) was analyzed using a colorimetric method employing 1,5-diphenylcarbazide (DPC) reagent.[34] The concentration of photogenerated H_2O_2 was determined by a colorimetric DPD method.[35] The absorption change was monitored at 540 nm ($\varepsilon = 6850$ M^{-1} cm^{-1})[36] for Cr(VI) and at 551 nm ($\varepsilon = 2 \times 10^4$ M^{-1} cm^{-1})[35] for H_2O_2 using a UV/Vis spectrophotometer (Agilent 8453).

The production of OH radicals was indirectly monitored using coumarin as a chemical trap, which is oxidatively converted into 7-hydroxycoumarin (7-HC) through the reaction with $^{\bullet}OH$ (coumarin + $^{\bullet}OH$ → 7-HC).[37] The hydroxylated product was quantified by measuring the fluorescence emission intensity at

460 nm under the excitation at 332 nm. For electron paramagnetic resonance (EPR) analysis, 5,5-dimethyl-1-pyrroline-*N*-oxide (DMPO) was used as a spin-trapping agent for OH radical. The EPR spectra of DMPO–OH were monitored using a JES-TE 300 spectrometer (JEOL, Japan). EPR was measured with the conditions of microwave power of 3 mW, microwave frequency of 9.42 GHz, center field 338.25 mT, modulation width of 0.2 mT, and modulation frequency of 100 kHz.

Photoelectrochemical (PEC) measurements

All PEC measurements were carried out in a conventional three-electrode cell using a computer-controlled potentiostat (Gamry, Reference 600). The PEC reactor was stirred and bubbled with nitrogen. The catalyst-coated photoanode, a Ag/AgCl (3.0 M NaCl) electrode and a Pt wire (when electrochemical impedance spectrum (EIS) was measured) or a graphite rod (when photocurrent was measured) were used as a working, a reference and a counter electrode, respectively. The working electrode was fabricated using Carbowax as a binder. TiO_2 powder was added in the solution of mixture of poly(ethylene glycol) (PEG, Aldrich, molecular weight: 20 kDa) and distilled water (50 wt%) and coated on a FTO plate using the doctor-blade method with tracks of two layers of Scotch tape. The TiO_2-coated electrode was calcined at 450 °C for 1 h, cooled to room temperature and then immersed into an acidic solution (pH 3) of dye (curcumin and RuL_3 were dissolved in ethanol and distilled water, respectively) over 12 h to prepare the dye-adsorbed TiO_2/FTO electrode. The photoanode was immersed in $NaClO_4$ solution and the potential bias was set at +0.6 V (*vs.* Ag/AgCl) during PEC measurements.

Results and discussion

Characterization of photocatalysts

The spectroscopic and electrochemical parameters of curcumin and Ru-dye are compared in Table 1. Because curcumin has a far more negative LUMO (lowest unoccupied molecular orbital) level than Ru-dye, the thermodynamic driving force for the electron transfer to the semiconductor conduction band (CB) should be higher compared to that of Ru-dye/TiO_2. The optical absorption properties of the curcumin/TiO_2 samples with various loadings of curcumin are represented by their diffuse reflectance spectra (Fig. 1). Bare TiO_2 cannot absorb visible light due to its large bandgap (~3.0 eV), and the visible light absorption of curcumin/TiO_2 increased with increasing curcumin concentration in the curcumin absorption spectral region, which confirms the successful loading of curcumin on the surface of TiO_2 nanoparticles.

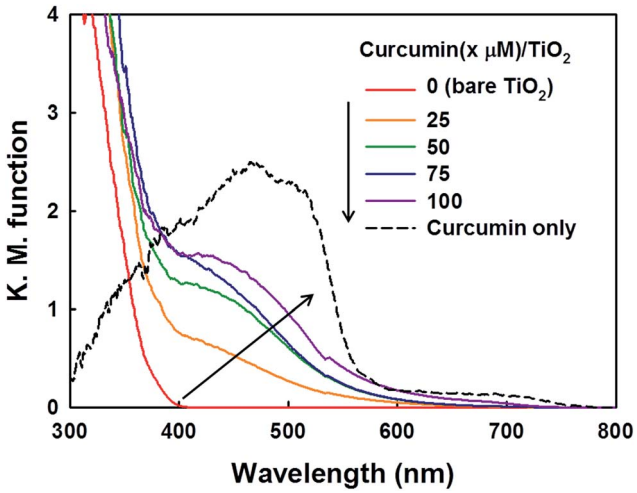

Fig. 1 Diffuse reflectance UV/visible spectra of bare TiO_2, curcumin, and curcumin/TiO_2.

To confirm the adsorption of curcumin on the TiO_2 surface, FT-IR spectra of curcumin/TiO_2 was compared with that of bare TiO_2 and curcumin powder. As shown in Fig. S1a,† the curcumin/TiO_2 sample exhibits two distinct peaks at 1691 cm^{-1} and 1507 cm^{-1}, which correspond to the C=O and C=C functional groups of curcumin, respectively.[38] This also confirms that curcumin is adsorbed on the TiO_2 surface. The C=O peak was slightly shifted to a higher wavenumber, which indicates that the β-diketone group in curcumin forms a chelate complex on the TiO_2 surface.[39] The adsorption of curcumin on TiO_2 was also corroborated through C 1s and O 1s XPS analysis (Fig. S1b and c†). The peak intensities corresponding to C=O (at 287.7 eV for C 1s and at 531.7 eV for O 1s), C–O (at 286.5 eV for C 1s and 533.2 eV for O 1s), and C–C (at 284.9 eV for C 1s)[40,41] considerably increased compared to bare TiO_2. Furthermore, the peaks at 288.6 eV for C 1s and 533.2 eV for O 1s corresponding to C–OH[6] newly appeared in curcumin/TiO_2. Lastly, the presence of organic carbons (curcumin) on the TiO_2 surface was confirmed by electron energy loss spectroscopy (EELS) mapping (Fig. S2†). The Ti species were clearly identified in both bare TiO_2 and curcumin/TiO_2 samples, whereas the C species was only observed in the curcumin/TiO_2 sample. All these spectroscopic and microscopic analyses confirm that curcumin is adsorbed on the TiO_2 surface through complexation as depicted in Scheme 1.

Table 1 Spectroscopic and electrochemical properties of curcumin and RuL_3

Dye	λ_{max}/nm	ε_{max}/M^{-1} cm^{-1}	ΔE^b/V	E^0(dye/dye$^{\bullet+}$)/V_{NHE}	E^0(dye*/dye$^{\bullet+}$)/V_{NHE}
Cur	424	48 000[a]	2.64	0.55[d]	−2.09[d]
RuL_3[c]	465	21 200	2.20	1.39	−0.81

[a] Ref. 51. [b] HOMO–LUMO gap. [c] Ref. 24. [d] Ref. 52.

Photochemical and photoelectrochemical activity tests under visible light

The photochemical activities of as-prepared samples were evaluated for the reduction of Cr(VI) to Cr(III) (less toxic form) and the degradation of DCA and TMA under visible light ($\lambda >$ 420 nm). First of all, the photochemical reduction of Cr(VI) with curcumin/TiO_2 was compared with that of bare TiO_2 and RuL_3/TiO_2 in the presence of ethanol as a hole scavenger. Although the adsorption of curcumin on TiO_2 surface steadily increased with increasing the concentration of curcumin up to 100 μM, the photochemical activity for Cr(VI) reduction was maximized at the curcumin concentration of 50 μM (Fig. 2a). Therefore, the curcumin concentration was fixed at 50 μM for all visible light activity tests. The control catalyst of RuL_3/TiO_2 was also prepared using the sensitizer concentration of 50 μM. Fig. 2b shows the time profiles of photochemical reduction of Cr(VI) in the visible light illuminated catalyst suspension. For the control experiments, the reduction of Cr(VI) was tested with curcumin only and bare TiO_2 under visible light and curcumin/TiO_2 in the dark condition. The visible light-sensitized reduction of Cr(VI) by curcumin only and the adsorption of Cr(VI) on curcumin/TiO_2 surface were negligible. The activity of bare TiO_2 was very low because of the lack of visible light absorption. When dye (curcumin or Ru-dye) was adsorbed on TiO_2 surface, the activity was markedly enhanced. This result is ascribed to fact that excitation of dye under visible light induced the transfer of photogenerated electrons to CB of TiO_2 and further reaction with Cr(VI). Since curcumin has a higher absorption coefficient of visible light and a more negative LUMO level than RuL_3 (Table 1), the electron transfer from dye LUMO to TiO_2 CB should be more efficient in curcumin/TiO_2 than RuL_3/TiO_2. As a result, the photochemical reduction of Cr(VI) is far more efficient with curcumin/TiO_2 than RuL_3/TiO_2. The wavelength-dependent activities for Cr(VI) reduction (Fig. 2c) are consistent with the dye absorption spectral profiles, which confirms the dye sensitization mechanism. The photoluminescence (PL) intensity of curcumin was completely quenched in the presence of TiO_2 (Fig. S3†), which further supports the dye sensitization mechanism on curcumin/TiO_2 under visible light.

Fig. 3 compares the time profiles of the photochemical degradation of DCA (with TOC removal) and TMA under visible light irradiation with bare TiO_2, RuL_3/TiO_2, and curcumin/TiO_2. For all cases, curcumin/TiO_2 exhibited the higher visible light activity than others, which is consistent with the photochemical reduction of Cr(VI) (see Fig. 2). This demonstrates that the curcumin/TiO_2 is efficient in the photooxidative conversion as well as the photoreductive conversion. The photochemical degradation of DCA and TMA with curcumin/TiO_2 was completely inhibited in the presence of excess *t*-BuOH (˙OH scavenger), which implies that OH radicals are involved as a major oxidant in this visible light-sensitized system. TMA is a very recalcitrant compound that can be degraded by OH radicals only,[42,43] and its successful degradation under visible light is a clear indication of OH radical generation through the sensitization process. Since the curcumin HOMO level (0.55 V_{NHE}) is not energetic enough to generate ˙OH (E^0(˙OH/H_2O) = 2.77 V_{NHE}), the generation of ˙OH in the sensitization system should be mediated by the reductive conversion of O_2 ($O_2 \rightarrow HO_2^{\cdot} \rightarrow H_2O_2 \rightarrow$ ˙OH).[44] To confirm the generation of ˙OH through the reduction of O_2, the production of intermediate H_2O_2 was confirmed (see Fig. 4a). When the suspension of curcumin/TiO_2 was purged with argon gas, H_2O_2 was not produced at all because of the

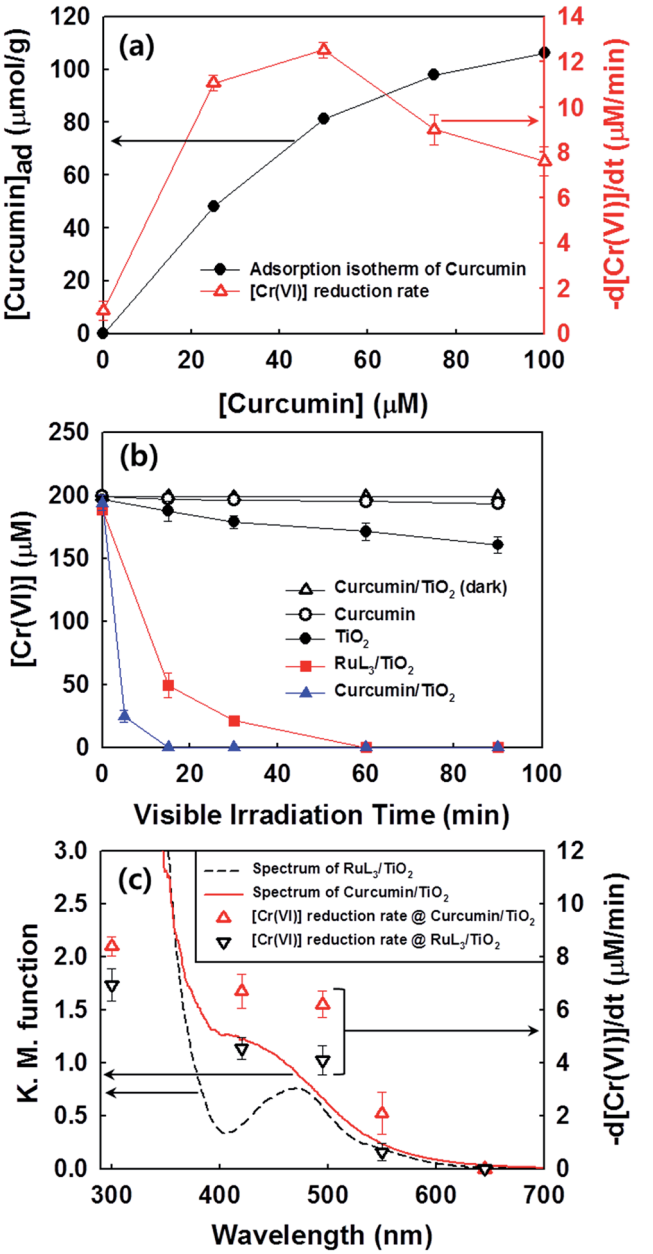

Fig. 2 (a) Visible light-sensitized reduction of Cr(VI) on TiO_2 as a function of the curcumin concentration and the adsorption isotherm of curcumin in the aqueous suspension of TiO_2. (b) Time profiles of visible light-induced removal of Cr(VI) in catalyst suspensions, and (c) the removal rates of Cr(VI) on dye/TiO_2 as a function of the irradiation wavelength. The diffuse reflectance spectra of curcumin/TiO_2 and RuL_3/TiO_2 are compared. The wavelength in the *x*-axis refers to the cutoff λ of the longpass filter (λ_{irrad} > cutoff λ). The experimental conditions were [catalyst] = 0.5 g L^{-1}, $[Cr(VI)]_0$ = 200 μM, $[EtOH]_0$ = 10 mM, pH_0 = 3.0, λ > 420 nm (for a and b), air-equilibrated for 30 min prior to irradiation.

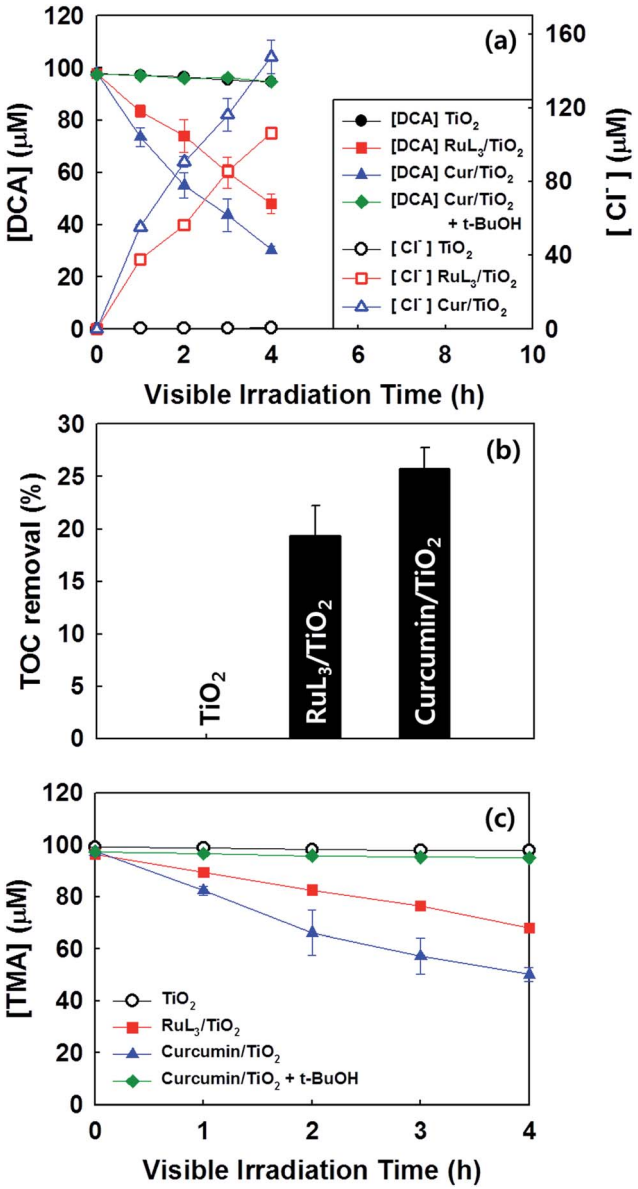

Fig. 3 (a) Visible light-sensitized degradation of DCA with the accompanying production of chloride, (b) TOC removal efficiencies after 4 h photodegradation of DCA, (c) visible light-sensitized degradation of TMA with bare TiO_2, RuL_3/TiO_2, and curcumin/TiO_2. The experimental conditions were [catalyst] = 0.5 g L^{-1}, $[DCA]_0 = [TMA]_0 =$ 100 μM, [*t*-BuOH] = 100 mM (for a and c), $pH_0 = 3.0$, $\lambda > 420$ nm, air-equilibrated for 30 min prior to irradiation.

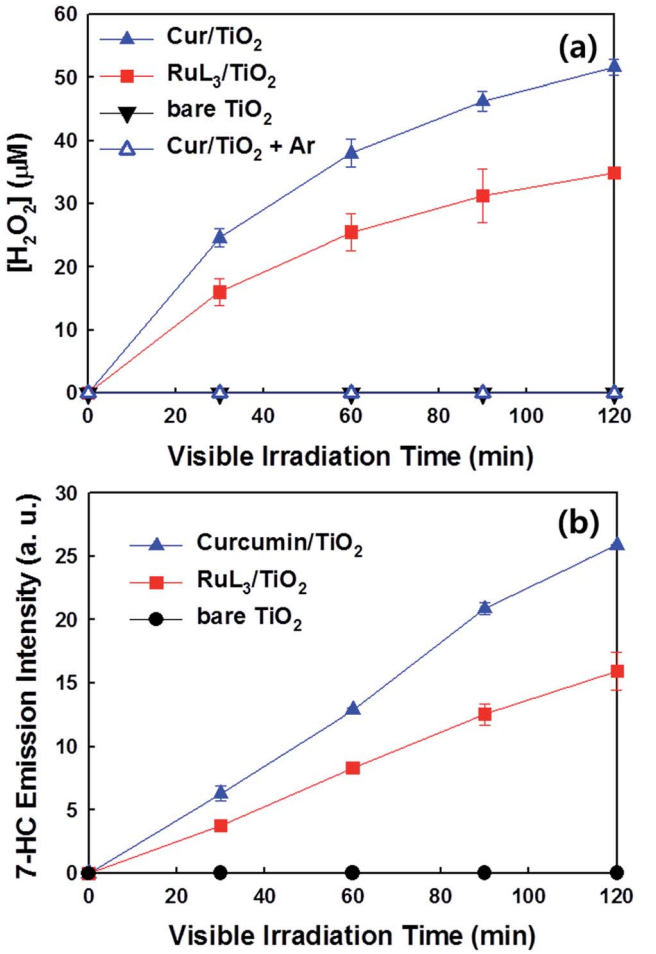

Fig. 4 Visible light-sensitized production of (a) H_2O_2 through O_2 reduction and (b) 7-hydroxycoumarin (7-HC) as a coumarin–OH adduct (monitored by its photoluminescence) in the illuminated catalyst suspensions. The experimental conditions were [catalyst] = 0.5 g L^{-1}, $[EtOH]_0 = 10$ mM (for a), $[coumarin]_0 = 1$ mM (for b), $pH_0 = 3.0$, $\lambda > 420$ nm, air-equilibrated for 30 min prior to irradiation except for the Ar-saturated case.

absence of O_2, which further confirms that H_2O_2 is generated *via* O_2 reduction. In addition, a chemical trapping of $^{\bullet}OH$ was tested as an indirect method of confirming the generation of $^{\bullet}OH$: the reaction of coumarin with $^{\bullet}OH$, which induces the formation of coumarin–OH adduct ($^{\bullet}OH$ + coumarin → 7-hydroxycoumarin (7-HC)), was monitored and quantitatively analyzed (see Fig. 4b). Fig. 4 compares the time profiles of the production of H_2O_2 and 7-HC with bare TiO_2, RuL_3/TiO_2, and curcumin/TiO_2 under visible light. The production of both H_2O_2 and 7-HC in curcumin/TiO_2 was higher than that in bare TiO_2 and RuL_3/TiO_2, which is consistent with the previous results shown in Fig. 2 and 3. The generation of $^{\bullet}OH$ in dye–TiO_2 composite was further detected using EPR spin-trapping technique (Fig. 5). The peaks of DMPO-OH in the EPR spectra were confirmed in the dye–TiO_2 composite after visible light irradiation for 5 min, which ensure the formation of $^{\bullet}OH$ *via* O_2 reduction.[45] In addition, the intensity of DMPO-OH peaks in curcumin/TiO_2 was higher than that in RuL_3/TiO_2. All results of the photo-activity tests confirmed the superior visible light activity of curcumin/TiO_2.

Furthermore, the PEC properties of curcumin/TiO_2 and RuL_3/TiO_2 electrodes were also compared. Fig. 6a shows the time profiles of photo-current generation using the electrodes of curcumin/TiO_2 and RuL_3/TiO_2 under visible light irradiation. The photocurrent obtained with curcumin/TiO_2 is significantly higher than that obtained with RuL_3/TiO_2. Furthermore, we measured the electrochemical impedance spectrum (EIS) to investigate the charge-transfer efficiency under visible light irradiation. As shown in Fig. 6b, the radius of the semicircle in the EIS spectra decreased in the order of bare TiO_2 > RuL_3/TiO_2

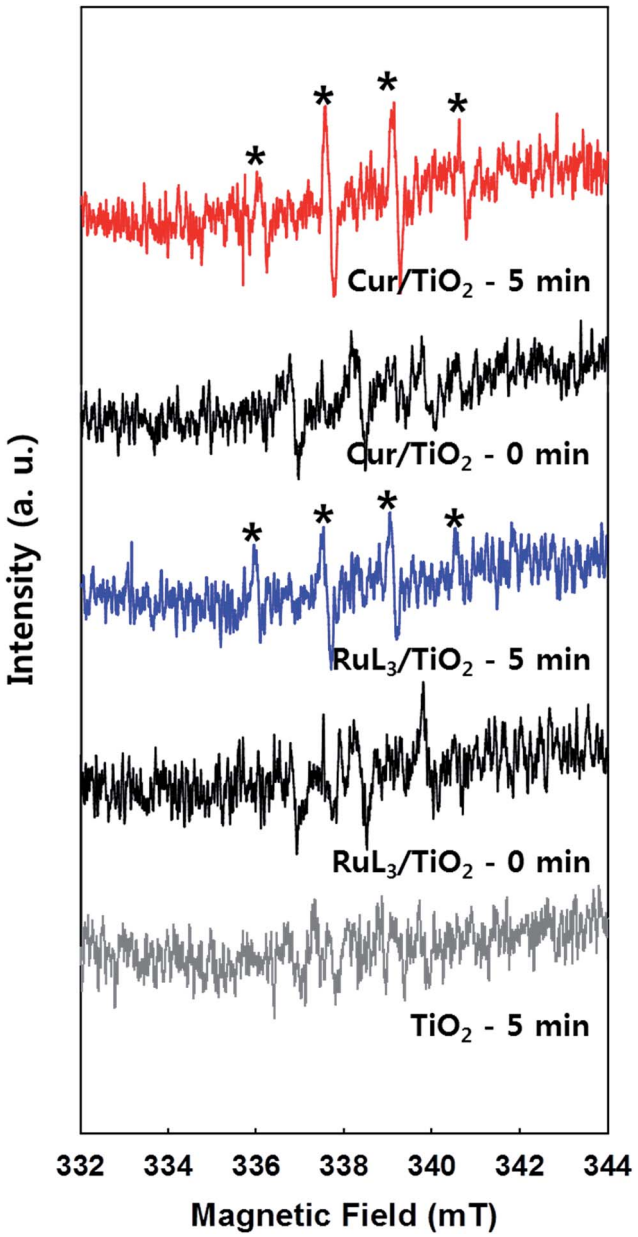

Fig. 5 EPR spectra of OH–DMPO (*) adducts in the illuminated catalyst suspension. The experimental conditions were [catalyst] = 1.5 g L^{-1}, $[DMPO]_0$ = 90 mM, pH_0 = 3.0, λ > 420 nm, air-equilibrated for 1 min prior to irradiation.

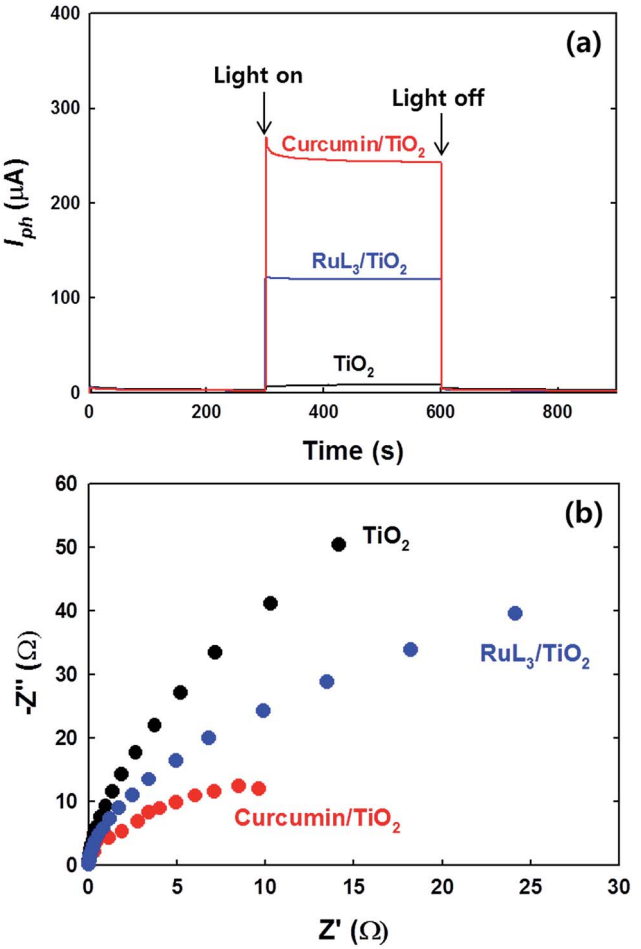

Fig. 6 (a) Photocurrent responses and (b) electrochemical impedance spectroscopic Nyquist plots of bare TiO_2, RuL_3/TiO_2, and curcumin/TiO_2 electrodes under visible light. The experimental conditions were $[NaClO_4]_0$ = 0.2 M, pH = 3.0, potential bias of +0.6 V (for a) and 0 V (for b) (*vs.* Ag/AgCl). The electrolyte solution was continuously N_2-purged.

> curcumin/TiO_2, which indicates that the interfacial charge-transfer resistance also decreased in the same order.[46] Both PEC results (Fig. 6a and b) indicate that the photo-induced electron transfer from the dye LUMO level to TiO_2 CB is more efficient in curcumin/TiO_2. Thus, the enhanced photochemical activity of curcumin/TiO_2 is ascribed not only to enhanced visible light absorption, but also to more efficient interfacial charge transfer.

pH-Dependent activity under visible light irradiation

In the case of RuL_3/TiO_2, the negatively charged RuL_3 (pK_a < 3) is anchored onto the positively charged TiO_2 surface through the carboxylate group. This binding mechanism is sensitive to pH change since the surface charge of TiO_2 changes from positive to negative above pH 6 (pH_{zpc} of TiO_2 ≈ 6).[37] The negative surface charge on TiO_2 hinders the adsorption of the anionic RuL_3 sensitizer. This electrostatic repulsion between the sensitizer and TiO_2 surface is the primary reason for lower stability of RuL_3/TiO_2 at pH > 6.[18] Fig. 7a shows that the adsorption of RuL_3 on TiO_2 steadily decreases from pH 3 to pH 9 while that of curcumin is much less affected by the pH change in the same condition, which indicates that the binding between curcumin and TiO_2 is only slightly affected by pH. Since curcumin is much less acidic than RuL_3 (pK_a ≈ 8.89),[47] the electrostatic repulsion between the negatively charged TiO_2 surface and the deprotonated curcumin should be significant only at pH > 9. As a result, the adsorption of curcumin is significantly higher than that of RuL_3 in the pH range of 3–9 (see Fig. 7a). Consequently, the photochemical and PEC activities of curcumin/TiO_2 are much less reduced when increasing pH from 3 to 9, whereas those of RuL_3/TiO_2 decreased significantly when pH increased above 6 (Fig. 7b and c). The curcumin/TiO_2 that

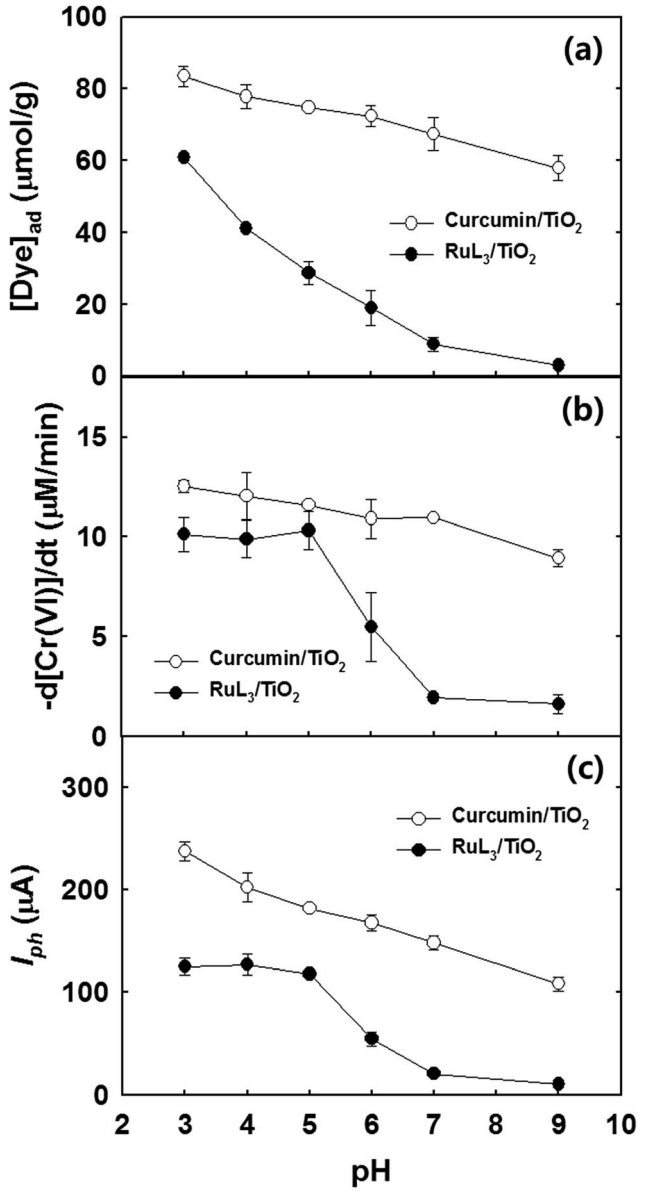

Fig. 7 pH-Dependent (a) adsorption isotherms of curcumin and RuL_3 in the aqueous suspension of TiO_2, (b) visible light-sensitized removal of Cr(VI), and (c) photocurrent generation on curcumin/TiO_2 and RuL_3/TiO_2 electrode. The experimental conditions were similar to those of Fig. 2 and 6.

employs an eco-friendly food dye as a sensitizer exhibits not only a higher photoactivity but also a higher stability in aquatic environment over a wide pH range.

The photostability of dye/TiO_2 was evaluated by repeating the cycles of DCA photodegradation using the same batch of catalyst (Fig. S4†). Each photodegradation cycle was carried out with using the dye/TiO_2 powder that was recovered from the previous cycle by filtering through 0.45 μm PTFE membrane, washing with distilled water, and the subsequent resuspension in a freshly prepared solution. Both curcumin and RuL_3 on TiO_2 exhibited serious deactivation during the repeated cycles of the photodegradation, which indicates that both dyes are degraded on TiO_2 under visible light. Although the dye-sensitized TiO_2 system has been often referred as "photocatalytic" in the literature,[48–50] it is hardly "catalytic" in reality because of the instability of dye itself. The degradation of organometallic dyes may release metal ions into water, which makes their application to water purification unsuitable. On the other hand, natural and edible dyes like curcumin are acceptable as a visible light sensitizer for water treatment purpose although they might be degraded and released into water.

Conclusions

The photochemical and PEC properties of curcumin-sensitized TiO_2 under visible light were investigated and compared with a well-known Ru–bipyridyl complex-sensitized TiO_2 system. The photochemical activities of curcumin/TiO_2 was much higher than those of RuL_3/TiO_2 for the reduction of Cr(VI), the degradation of organic compounds, and the production of hydroxyl radicals and H_2O_2 through O_2 reduction. As for the PEC properties, curcumin/TiO_2 electrode exhibited higher photocurrent generation and significantly lower charge transfer resistance compared to the RuL_3/TiO_2 electrode system. More importantly, the adsorption of curcumin on the TiO_2 surface and the resulting photo-activity were consistently higher than those of RuL_3/TiO_2 over a wide pH range. Therefore, the use of naturally-occurring, cheap and non-toxic curcumin as a sensitizer offers a practically viable method of TiO_2 activation under visible light for various solar environmental applications. However, it should be noted that the curcumin/TiO_2 like other dye-sensitized TiO_2 is not catalytic and stable at all and the dyes are degraded as a result of the sensitizing reactions in water. The curcumin dye should be considered as a sensitizing reagent which can be consumed as a result of photochemical reactions.

Acknowledgements

This work was supported by Global Research Laboratory (GRL) Program (NRF-2014K1A1A2041044) and KCAP (Sogang Univ.) (2009–0093880), which were funded by the Korea Government (MSIP) through the National Research Foundation (NRF).

References

1 H. Park, H.-i. Kim, G.-h. Moon and W. Choi, *Energy Environ. Sci.*, 2016, **9**, 8261–8272.
2 T. Tachikawa and T. Majima, *Chem. Soc. Rev.*, 2010, **39**, 4802–4819.
3 M. R. Hoffmann, S. T. Martin, W. Choi and D. W. Bahnemann, *Chem. Rev.*, 1995, **95**, 69–96.
4 Y. M. Huo, Z. F. Bian, X. Y. Zhang, Y. Jin, J. Zhu and H. X. Li, *J. Phys. Chem. C*, 2008, **112**, 6546.
5 G. Wu, T. Nishikawa, B. Ohtani and A. Chen, *Chem. Mater.*, 2007, **19**, 4530–4537.
6 J. Lim, D. Monllor-Satoca, J. S. Jang, S. Lee and W. Choi, *Appl. Catal., B*, 2014, **152–153**, 233–240.
7 J. B. Yin and X. P. Zhao, *Chem. Mater.*, 2004, **16**, 321–328.

8 H. Yu, X. J. Li, S. J. Zheng and W. Xu, *Mater. Chem. Phys.*, 2006, **97**, 59–63.
9 P. Wang, B. Huang, Y. Dai and M. H. Wangbo, *Phys. Chem. Chem. Phys.*, 2012, **14**, 9813–9825.
10 S. Linic, P. Christopher and D. B. Ingram, *Nat. Mater.*, 2011, **10**, 911–921.
11 A. Mikolajczyk, A. Malankowska, G. Nowaczyk, A. Gajewicz, S. Hirano, S. Jurga, A. Zaleska-Medynska and T. Puzyn, *Environ. Sci.: Nano*, 2016, **3**, 1425–1435.
12 H.-i. Kim, J. Kim, W. Kim and W. Choi, *J. Phys. Chem. C*, 2011, **115**, 9797–9805.
13 B. Liu, Y. Xue, J. Zhang, B. Han, J. Zhang, X. Suo, L. Mu and H. Shi, *Environ. Sci.: Nano*, 2017, **4**, 255–264.
14 J. Zhang, Y. Wang, J. Jin, J. Zhang, Z. Lin, F. Huang and J. Yu, *ACS Appl. Mater. Interfaces*, 2013, **5**, 10317–10324.
15 J. Yu, J. Zhang and M. Jaroniec, *Green Chem.*, 2010, **12**, 1611–1614.
16 G. Li, D. Zhang and J. C. Yu, *Environ. Sci. Technol.*, 2009, **43**, 7079–7085.
17 K. L. V. Joseph, J. Lim, A. Anthonysamy, H. Kim, W. Choi and J. K. Kim, *J. Mater. Chem. A*, 2015, **3**, 232–239.
18 Y. Park, S.-H. Lee, S. O. Kang and W. Choi, *Chem. Commun.*, 2010, **46**, 2477–2479.
19 Y. Park, W. Kim, D. Monllor-Satoca, T. Tachikawa, T. Majima and W. Choi, *J. Phys. Chem. Lett.*, 2013, **4**, 189–194.
20 J. Park, J. Yi, T. Tachikawa, T. Majima and W. Choi, *J. Phys. Chem. Lett.*, 2010, **1**, 1351–1355.
21 W. Kim, T. Tachikawa, T. Majima and W. Choi, *J. Phys. Chem. C*, 2009, **113**, 10603–10609.
22 A. Hagfeldt, G. Boshloo, L. Sun, L. Kloo and H. Pettersson, *Chem. Rev.*, 2010, **110**, 6595–6663.
23 E. Bae and W. Choi, *J. Phys. Chem. B*, 2006, **110**, 14792–14799.
24 H. Park, E. Bae, J.-J. Lee, J. Park and W. Choi, *J. Phys. Chem. B*, 2006, **110**, 8740–8749.
25 A. Mishra, M. K. R. Fischer and P. Bäuerle, *Angew. Chem., Int. Ed.*, 2009, **48**, 2474–2499.
26 Y. Wu, M. Marszalek, S. M. Zakeeruddin, Q. Zhang, H. Tian, M. Grätzel and W. Zhu, *Energy Environ. Sci.*, 2012, **5**, 8261–8272.
27 K. I. Priyadarsini, *J. Photochem. Photobiol., C*, 2009, **10**, 81–95.
28 B. B. Aggarwal, A. Kumar and A. C. Bharti, *Anticancer Res.*, 2003, **23**, 363–398.
29 R. A. Sharma, A. J. Gescher and W. P. Steward, *Eur. J. Cancer*, 2005, **41**, 1955–1968.
30 P. Anand, A. B. Kunnumakkara, R. A. Newman and B. B. Aggarwal, *Mol. Pharmaceutics*, 2007, **4**, 807–818.
31 H. Hatcher, R. Planalp, J. Cho, F. M. Torti and S. V. Torti, *Mol. Life Sci.*, 2008, **65**, 1631–1652.
32 N. Khan, F. Afaq and H. Mukhtar, *Antioxid. Redox Signaling*, 2008, **10**, 476.
33 T. Ganesh, J. H. Kim, S. J. Yoon, B. Kil, N. N. Maldar and J. W. Han, *Mater. Chem. Phys.*, 2010, **123**, 62–66.
34 *Standard Methods for the Examination of Water and Wastewater (20th ed.)*, ed. L. S. Clesceri, A. E. Greenberg and A. D. Eaton, American Public Health Association, Washington, DC, 1998.
35 H. Bader, V. Sturzenegger and J. Hoigne, *Water Res.*, 1988, **22**, 1109–1115.
36 J. Lim, P. Murugan, N. Lakshminarasimhan, J. Y. Kim, J. S. Lee, S.-H. Lee and W. Choi, *J. Catal.*, 2014, **310**, 91–99.
37 J. Kim, C. W. Lee and W. Choi, *Environ. Sci. Technol.*, 2010, **44**, 6849–6854.
38 S. Kundu and U. Nithiyanantham, *RSC Adv.*, 2013, **3**, 25278–25290.
39 B. Zebib, Z. Mouloungui and V. Noirot, *Bioinorg. Chem. Appl.*, 2010, **2010**, 1–8.
40 D. Yang, A. Velamakanni, G. Bozoklu, S. Park, M. Stoller, R. D. Piner, S. Stankovich, I. Jung, D. A. Field, C. A. Ventrice Jr and R. S. Ruoff, *Carbon*, 2009, **47**, 145–152.
41 R. He, X. Hu, H. C. Tan, J. Feng, C. Steffi, K. Wang and W. Wang, *J. Mater. Chem. B*, 2015, **3**, 2137–2146.
42 S. Kim and W. Choi, *Environ. Sci. Technol.*, 2002, **36**, 2019–2025.
43 S. Kim, S.-J. Hwang and W. Choi, *J. Phys. Chem. B*, 2005, **109**, 24260–24267.
44 H. Park, Y. Park, W. Kim and W. Choi, *J. Photochem. Photobiol., C*, 2013, **15**, 1–20.
45 J. Lim, H. Kim, P. J. J. Alvarez, J. Lee and W. Choi, *Environ. Sci. Technol.*, 2016, **50**, 10545–10553.
46 N. Lakshminarasimhan, A. D. Bokare and W. Choi, *J. Phys. Chem. C*, 2012, **116**, 17531–17539.
47 Z. Wang, M. H. M. Leung, T. W. Kee and D. S. English, *Langmuir*, 2009, **26**, 5520–5526.
48 P. Chowdhury, J. Moreira, H. Gomaa and A. K. Ray, *Ind. Eng. Chem. Res.*, 2012, **51**, 4523–4532.
49 J. Moon, C. Y. Yun, K.-W. Chung, M.-S. Kang and J. Yi, *Catal. Today*, 2003, **87**, 77–86.
50 M. S. Dieckmann and K. A. Gray, *Water Res.*, 1996, **30**, 1169–1183.
51 A. Dayton, K. Selvendiran, M. L. Kuppusamy, B. K. Rivera, S. Meduru, T. Kálai, K. Hideg and P. Kuppusamy, *Cancer Biol. Ther.*, 2010, **10**, 1027–1032.
52 U. Singh, S. Verma, H. N. Ghosh, M. C. Rath, K. I. Priyadarsini, A. Sharma, K. K. Pushpa, S. K. Sarkar and T. Mukherjee, *J. Mol. Catal. A: Chem.*, 2010, **318**, 106–111.